PIEZOELECTRIC MULTIFUNCTIONAL COMPOSITES DAMAGE DETECTION USING THEIR MODAL EFFECTIVE ELECTROMECHANICAL COUPLING

A. Benjeddou[a*], M. Hamdi[b]

[a]*Institut Supérieur de Mécanique de Paris, 3 rue Fernand Hainaut, 93400 Saint Ouen, France*
[b]*Institut Supérieur des Sciences Appliquées et de Technologie, 2112 Gafsa-Zarroug, Tunisia*
**benjeddou@supmeca.fr*

Keywords: piezoelectric multifunctional composites, damage detection, modal effective electromechanical coupling, finite element analysis.

Abstract
The present contribution focuses on the potential use of the so-called modal effective electro-mechanical coupling coefficient (EMCC) as a vibration-based damage indicator in piezoelectric (PE) laminated composites. For this purpose, three-dimensional piezoelectric fully coupled finite element analyses under four mechanical and two electrical boundary conditions are first conducted for healthy PE glass/carbon fiber reinforced composite beams and all types of vibration modes; then, two damage scenarios of a delamination and a notch (or crack) are considered for the EMCC change factor (ECF) assessment, under fixed damage characteristics (position, length, depth), as a damage indicator. Next, the latter is further assessed via a parametric analysis. It is found that the ECF is a better damage indicator for the out-of-plane bending modes than the frequency change factor.

1. Introduction

Vibration-based damage identification (VBDI) for structural health monitoring (SHM) is a well-established technique for passive and active structures [1]. However, except few works [2-4], the use of piezoelectric (PE) transducers as sensors or/and actuators was mainly limited to Lamb waves [5] and impedance [6] based *high frequency* approaches. On the other hand, the material *electromechanical coupling factor* (EMCF) is a measure of the conversion efficiency of electrical energy to mechanical one and vice-versa [7]. Therefore, since any change in the host structure stiffness or mass, due to the damage, considerably affects the energy conversion of the piezoelectric devices, the so-called modal effective (structural) *electromechanical coupling coefficient* (EMCC) was shown earlier to be a potential good candidate for damage detection in piezoelectric multifunctional composites [8]. Until now this idea was investigated only for composite beams using *one-dimensional* (1D) uncoupled [8] or coupled [9] finite elements (FE); hence, only out of the FE model plane bending modes were accessible. It is then the objective of the present contribution to focus on the modal effective EMCC as a vibration (*low-frequency*) based damage indicator for its use in SHM of piezoelectric multifunctional composites. For this purpose, now *three-dimensional* (3D) PE fully coupled FE analyses under four mechanical (clamped-free CF, clamped-clamped CC, clamped-supported CS and supported-supported SS) and two electrical (short-circuit, *sc*, and

open-circuit, *oc*, electrodes of the piezoceramic patches) boundary conditions (BC) are first conducted for assessing their effects on the modal effective EMCC of healthy piezoelectric glass/carbon fiber reinforced (GFRP/CFRP) hybrid composite beams for all types of vibration modes (transverse and in-plane bending, and torsion); then, two damage scenarios of a delamination, modeled by the *removal of material* (RM), and a notch (or crack), modeled by the *inclusion of a soft layer* (ISL) are considered for the *EMCC change factor* (ECF) assessment, under *fixed damage characteristics* (position, length and depth), as a damage indicator. Next, the latter is further assessed via a *parametric analysis* on the previous damage key parameters under above four mechanical and two electrical BC.

2. Modal effective EMCC-based damage indicators

As a potential damage indictor, the modal effective EMCC (*K*) has been first proposed in this approximate (*a*) form in terms of the PE material EMCF (*k*) and the modal stiffness matrices of the host structure (*hs*), $\hat{K}_{hs}$, and that with *shorted* (*E*) PE patches (*hs+piezos*), $\hat{K}^{E}_{hs+piezos}$ [8]:

$$K_a^2 = \left(1 - \frac{\hat{K}_{hs}}{\hat{K}^{E}_{hs+piezos}}\right)\left(\frac{k^2}{1-k^2}\right) \tag{1}$$

While this approximation is very easy to use since it does not require special coupled piezoelectric numerical tools like FE ones, it has a major drawback that it cannot handle the physical *equipotential* (EP) constraints on the nodal electric potential degrees of freedom (DOFs) of the patches' electrodes in order to fulfill the electric potential spatial uniformity. This motivated revisiting this indicator by developing a special coupled PE beam FE with nodal electric potential DOFs that enable enforcing the EP constraints on the patches' electrodes; it allowed also to use either of these definitions of the modal effective EMCC [9]:

$$K_{oc}^2 = \frac{f_{oc}^2 - f_{sc}^2}{f_{oc}^2},\ K_{sc}^2 = \frac{f_{oc}^2 - f_{sc}^2}{f_{sc}^2} \tag{2a,b}$$

The first definition is generally used when *oc* and *sc* are approximated from poles (resonances) and zeros (anti-resonances) of the electric impedance transfer function, while the second definition is generally used when *oc* and *sc* frequencies are extracted from vibration (modal) analyses. These definitions are linked via this expression [10]:

$$K_{oc}^2 = \frac{K_{sc}^2}{K_{sc}^2 + 1} \tag{3}$$

Hence, if $K_{sc}^2 \ll 1$ both EMCCs are approximately equal. Since this approximation is damage dependent, both expressions are used for defining the *EMCC change factor* (ECF^2) [9]:

$$ECF_{oc}^2(\%) = 100 \times \frac{\left(K_{oc}^2\right)_h - \left(K_{oc}^2\right)_d}{\left(K_{oc}^2\right)_h},\ ECF_{sc}^2(\%) = 100 \times \frac{\left(K_{sc}^2\right)_h - \left(K_{sc}^2\right)_d}{\left(K_{sc}^2\right)_h} \tag{4a,b}$$

In order to assess above ECF^2 damage indication performance, these *frequency change factors* (*FCF*) that use *squared* frequencies, which were introduced first in [9] and revisited recently in [11], are here used for comparison purpose:

$$FCF_{oc}^2(\%) = 100 \times \frac{\left(f_{oc}^2\right)_h - \left(f_{oc}^2\right)_d}{\left(f_{oc}^2\right)_h},\ FCF_{sc}^2(\%) = 100 \times \frac{\left(f_{sc}^2\right)_h - \left(f_{sc}^2\right)_d}{\left(f_{sc}^2\right)_h} \qquad (5a,b)$$

Worthy to stress that, in [9], the numerators of (4a,b) had opposite signs (*d-h* instead of *h-d* here). Besides, in [8], the EMCC square root and *sc* only *simple* frequencies have been used. To highlight such difference, a subscript 2 is used here for FCFs defined in (5).

3. Damage influence on the EMCC change factors

The benchmark used for the assessment of above modal effective EMCC-based damage indicators is that proposed in [8] and used recently in [11]; it consists of a 32-ply symmetric composite cantilever beam with dimensions $L \times B \times H = 200 \times 20 \times 4$ mm^3 and stacking sequence of $[\mathbf{0}_4/90_8/0_4]_S$, where bold plies are made of GFRP, while the others are in CFRP. Two piezoceramic (PZT-5A) patches, polarized along their thickness and of dimensions $L_a \times B \times H_a = 25 \times 20 \times 0.5$ mm^3, are placed in replacement of bottom and top four 90°-plies at the length position of $X_a = 22.5$ mm from the beam left end. The sketched geometrical model shown in Fig. 1 is modeled within ANSYS® and meshed using 3D quadratic (20 nodes) elastic (displacement) SOLID191 and fully coupled piezoelectric SOLID226 (displacement-potential) FE for composite and piezoelectric layers, respectively (Fig. 2). The FE mesh has 4480 elements and 21879 nodes (see [11] for detailed FE subdivisions and materials data).

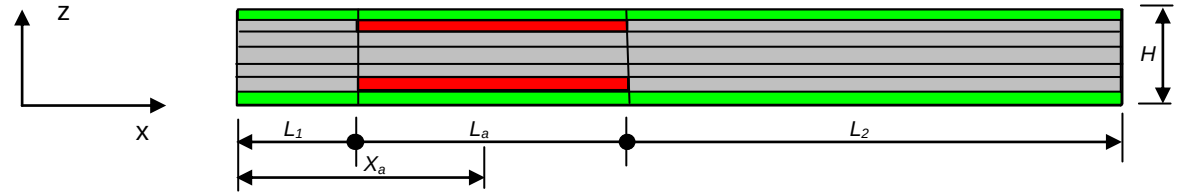

Figure 1. Smart hybrid laminated composite beam sketch (red: PZT-5A, green: GFRP, gray: CFRP).

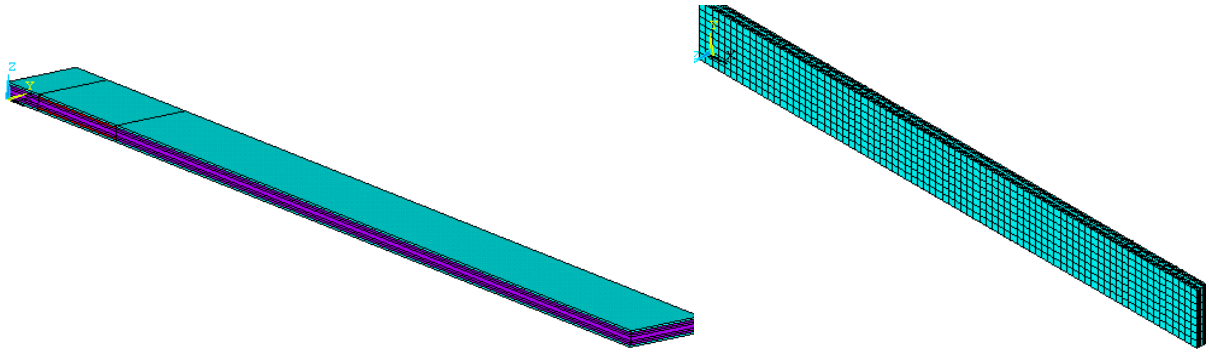

Figure 2. Smart hybrid laminated composite beam geometric (left) and FE (right) 3D models.

Two types of damages are considered; the first simulates a notch or crack that is modeled by the removal of corresponding material, while the second simulates a delamination that is modeled by an inclusion of a soft layer made of a thin Teflon® film. The corresponding geometrical sketches are shown in Fig. 3 and their meshes, as shown in Fig. 4, have 4432 elements and 21747 nodes for the RM model, and 4480 elements and 21879 nodes for the ISL one (see [11] for details of their FE meshes).

Worthy to mention that clamping is obtained by fixing the FE three displacements (translations) DOFs to zero values, while simply-supported condition is modeled here by letting free only the axial displacement (translation) DOF.

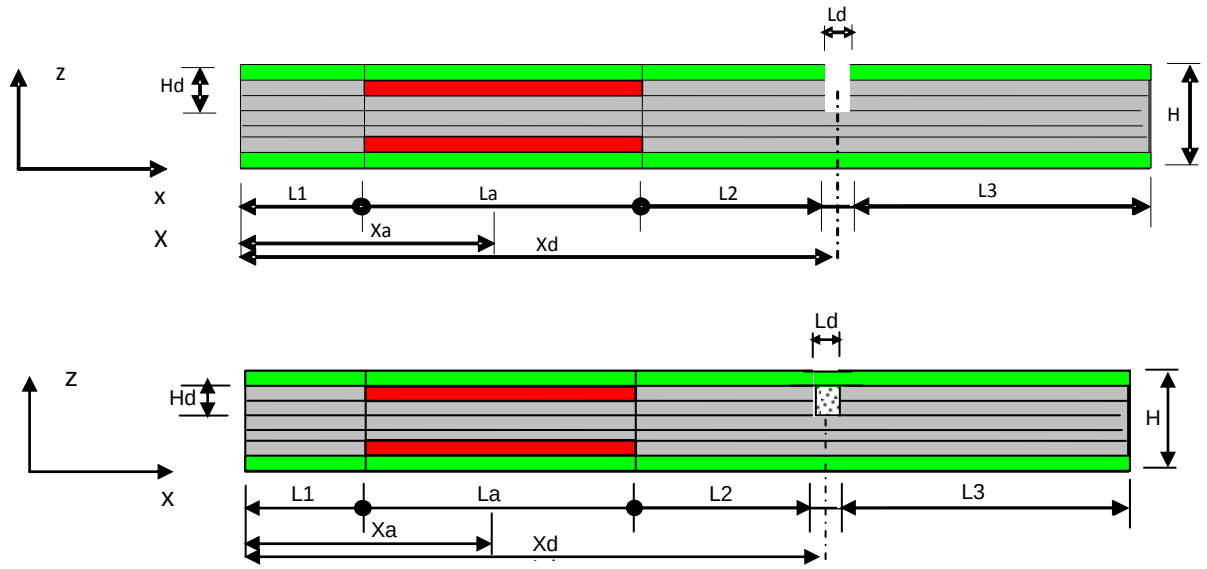

Figure 3. RM (top) and ISL (bottom) damaged smart beam (red: PZT-5A, green: GFRP, gray: CFRP).

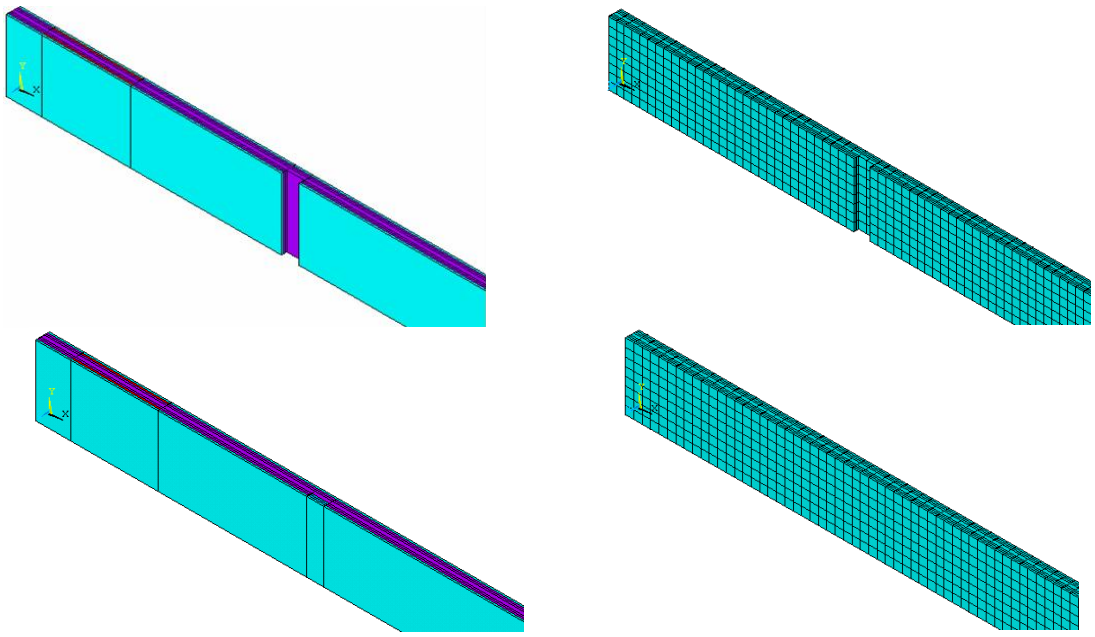

Figure 4. RM (top) and ISL (bottom) damaged smart beam geometric (left) and FE (right) 3D models.

The FE simulations have been conducted for the healthy and damaged (RM and ISL) smart hybrid laminated composite beams under four mechanical BC (CF, CS, CC, SS) and two electrical connections (*sc*, *oc*). The obtained results are shown in Table 1, where zero EMCC values indicate electromechanically uncoupled modes (% hundredths are only numerical). From the results, it can be observed that (i) only the RM damage changes the modes types (for only the CF BC); (ii) the modes' electromechanical coupling is not affected by the damage since the healthy uncoupled *x-y in-plane bending* and *torsion* modes remain uncoupled for the damaged (RM and ISL) beams; hence, only the transverse (x-z) bending modes are coupled and affected by the damage; (iii) in contrary to the RM damage model, the ISL one does not affect the modes order and type for all BC; care should be then taken when using RM model for the damage simulation under CF BC since it affects the modes types and order (see modes 2, 3, 7, 8 of this case); (iv) the CS, CC and SS BC have different modes' types than the CF one. Besides, the SS BC case has different 3rd and 4th modes' types than CS and CC BC which

have the same modes' types. Hence, it appears clearly that the popular numerical CF and analytical SS BC are not the best ones for studying theoretically (numerically or analytically) the VBDI performance in 3D modeling; the latter is the realistic way of simulating actual damaged structures which have intrinsically a 3D response; the best BCs from this point of view are then CS and CC, with a preference to the latter due to its practical interest. Finally, with the current patches' position and damage characteristics, the highest effective EMCC is obtained for the first x-z bending mode for all BCs except SS. Also, as expected, the *sc* EMCCs are higher than *oc* ones; the former are then more suitable for damage indication.

	Mode	Healthy K^2 (%)			RM K^2 (%)			ISL K^2 (%)		
BC	**order**	**Type**	**SC**	**OC**	**Type**	**SC**	**OC**	**Type**	**SC**	**OC**
CF	1	f_{xz}^1	1.65	1.63	f_{xz}^1	1.55	1.53	f_{xz}^1	1.39	1.37
	2	f_{xy}^1	**0.00**	**0.00**	f_{xz}^2	0.64	0.64	f_{xy}^1	**0.00**	**0.00**
	3	f_{xz}^2	0.55	0.55	f_{xy}^1	**0.00**	**0.00**	f_{xz}^2	0.48	0.47
	4	t^1	**0.00**	**0.00**	t^1	**0.00**	**0.00**	t^1	**0.00**	**0.00**
	5	f_{xz}^3	0.04	0.04	f_{xz}^3	0.05	0.05	f_{xz}^3	0.04	0.04
	6	t^2	**0.00**	**0.00**	t^2	**0.00**	**0.00**	t^2	**0.00**	**0.00**
	7	f_{xy}^2	**0.00**	**0.00**	f_{xz}^4	0.15	0.14	f_{xy}^2	**0.00**	**0.00**
	8	f_{xz}^4	0.13	0.13	f_{xy}^2	**0.00**	**0.00**	f_{xz}^4	0.12	0.12
CS	1	f_{xz}^1	0.79	0.78	f_{xz}^1	0.86	0.85	f_{xz}^1	0.67	0.67
	2	f_{xz}^2	0.13	0.13	f_{xz}^2	0.13	0.13	f_{xz}^2	0.09	0.09
	3	t^1	**0.00**	**0.00**	t^1	**0.00**	**0.00**	t^1	**0.00**	**0.00**
	4	f_{xy}^1	**0.00**	**0.00**	f_{xy}^1	**0.00**	**0.00**	f_{xy}^1	**0.00**	**0.00**
	5	f_{xz}^3	0.05	0.05	f_{xz}^3	0.06	0.06	f_{xz}^3	0.05	0.05
	6	t^2	**0.00**	**0.00**	t^2	**0.00**	**0.00**	t^2	**0.00**	**0.00**
	7	f_{xz}^4	0.40	0.40	f_{xz}^4	0.37	0.37	f_{xz}^4	0.35	0.35
	8	t^3	**0.00**	**0.00**	t^3	**0.00**	**0.00**	t^3	**0.00**	**0.00**
CC	1	f_{xz}^1	0.59	0.58	f_{xz}^1	0.66	0.65	f_{xz}^1	0.50	0.50
	2	f_{xz}^2	0.04	0.04	f_{xz}^2	0.04	0.04	f_{xz}^2	0.04	0.04
	3	t^1	**0.00**	**0.00**	t^1	**0.00**	**0.00**	t^1	**0.00**	**0.00**
	4	f_{xy}^1	**0.00**	**0.00**	f_{xy}^1	**0.00**	**0.00**	f_{xy}^1	**0.00**	**0.00**
	5	f_{xz}^3	0.13	0.13	f_{xz}^3	0.14	0.14	f_{xz}^3	0.11	0.11
	6	t^2	**0.01**	**0.01**	t^2	**0.00**	**0.00**	t^2	**0.01**	**0.01**
	7	f_{xz}^4	0.47	0.47	f_{xz}^4	0.41	0.41	f_{xz}^4	0.42	0.41
	8	t^3	**0.00**	**0.00**	t^3	**0.00**	**0.00**	t^3	**0.00**	**0.00**
SS	1	f_{xz}^1	0.14	0.14	f_{xz}^1	0.12	0.12	f_{xz}^1	0.12	0.12
	2	f_{xz}^2	0.55	0.55	f_{xz}^2	0.49	0.49	f_{xz}^2	0.46	0.46
	3	f_{xy}^1	**0.00**	**0.00**	f_{xy}^1	**0.00**	**0.00**	f_{xy}^1	**0.00**	**0.00**
	4	t^1	**0.00**	**0.00**	t^1	**0.00**	0.00	t^1	**0.00**	**0.00**
	5	f_{xz}^3	0.95	0.94	f_{xz}^3	1.05	1.04	f_{xz}^3	0.79	0.78
	6	t^2	**0.01**	**0.01**	t^2	**0.00**	**0.00**	t^2	**0.00**	**0.00**
	7	f_{xz}^4	1.01	1.00	f_{xz}^4	0.91	0.91	f_{xz}^4	0.88	0.87
	8	t^3	**0.00**	**0.00**	t^3	**0.00**	**0.00**	t^3	**0.00**	**0.00**

Table 1. First 8 modes *squared* EMCC, K^2 (%), of healthy and damaged smart hybrid composite beams.

Table 2 provides *sc* and *oc* percent FCF^2 and ECF^2. It can be noticed for the former that: (i) due to the more structural degradation, RM indicator has much higher values than ISL one; (ii) RM indicator is mostly positive, while ISL one is mostly negative, indicating that in

contrary to the RM damage which decreases the healthy frequencies, the ISL damage increases them; (iii) *oc* and *sc* indicators highest values (in bold) are obtained for transverse (x-z) bending modes under all BC for RM damage, but for the first in-plane (x-y) bending mode for the ISL damage under all BC, except the SS case; (iv) *sc* and *oc* FCF^2 maximum values are slightly different for the RM damage model but are almost similar for the ISL one.

Damage model		**RM**				**ISL**			
	Mode	**FCF^2 (%)**		**ECF (%)**		**FCF^2 (%)**		**ECF (%)**	
BC	**type**	**SC**	**OC**	**SC**	**OC**	**SC**	**OC**	**SC**	**OC**
CF	f_{xz}^1	5.29	**5.38**	5.92	5.83	-1.11	-0.85	**15.96**	**15,74**
	f_{xy}^1	1.08	1.08	0.00	0.00	**-2.17**	**-2.17**	0.00	0,00
	f_{xz}^2	**5.42**	5.34	-15.79	-15.69	-1.45	-1.37	13.85	13,78
	t^1	5.05	5.04	0.00	0.00	0.60	0.60	0.00	0,00
	f_{xz}^3	3.07	3.06	**-35.44**	**-35.42**	-0.60	-0.60	0.30	0,30
	t^2	-1.41	-1.41	0.00	0.00	-1.32	-1.32	0.00	0,00
	f_{xy}^2	-0.20	-0.20	0.00	0.00	-1.58	-1.58	0.00	0,00
	f_{xz}^4	2.72	2.70	-12.07	-12.05	-0.48	-0.46	10.74	10,73
CS	f_{xz}^1	1.85	1.77	-9.16	-9.08	-1.38	-1.26	14.98	14,88
	f_{xz}^2	5.34	5.34	-2.78	-2.78	-1.07	-1.04	**25.41**	**25,38**
	t^1	0.53	0.53	0.00	0.00	-0.71	-0.71	0.00	0,00
	f_{xy}^1	-0.09	-0.09	0.00	0.00	**-1.48**	**-1.48**	0.00	0,00
	f_{xz}^3	0.85	0.84	**-14.77**	**-14.77**	-0.11	-0.11	0.05	0,05
	t^2	1.40	1.40	0.00	0.00	-0.42	-0.42	0.00	0,00
	f_{xz}^4	**6.47**	**6.49**	6.45	6.43	-1.44	-1.39	12.54	12,50
	t^3	3.59	3.59	0.00	0.00	0.30	0.30	0.00	0,00
CC	f_{xz}^1	3.46	3.40	-11.92	-11.84	-1.65	-1.57	14.76	14,68
	f_{xz}^2	3.28	3.28	-1.68	-1.68	-0.58	-0.58	0.29	0,29
	t^1	-0.02	-0.02	0.00	0.00	-0.91	-0.91	0.00	0,00
	f_{xy}^1	-0.82	-0.82	0.00	0.00	**-1.69**	**-1.69**	0.00	0,00
	f_{xz}^3	2.59	2.59	-6.66	-6.65	-0.45	-0.43	**15.98**	**15,97**
	t^2	2.53	2.54	0.00	0.00	-0.08	-0.08	0.00	0,00
	f_{xz}^4	**5.31**	**5.37**	**12.19**	**12.14**	-1.29	-1.23	11.49	11,44
	t^3	3.01	3.01	0.00	0.00	0.01	0.01	0.00	0,00
SS	f_{xz}^1	**8.58**	**8.60**	**12.85**	**12.83**	-1.10	-1.07	**17.13**	**17,11**
	f_{xz}^2	2.77	2.83	10.86	10.80	-0.70	-0.61	16.06	15,99
	f_{xy}^1	0.05	0.05	0.00	0.00	-1.31	-1.31	0.00	0,00
	t^1	-0.10	-0.10	0.00	0.00	-0.92	-0.92	0.00	0,00
	f_{xz}^3	3.50	3.40	-10.72	-10.61	-1.18	-1.02	17.03	16,89
	t^2	3.26	3.27	0.00	0.00	0.06	0.06	0.00	0,00
	f_{xz}^4	5.35	5.44	9.55	9.46	**-1.59**	**-1.46**	12.70	12,59
	t^3	2.74	2.74	0.00	0.00	-0.52	-0.52	0.00	0,00

Table 2. First 8 modes *squared* FCF (%) and ECF (%) of MR and ISL damaged smart hybrid composite beams.

For the ECF^2 indicators, it is found that they are much more performant (having much higher values) for indicating both RM and ISL damages than the FCF^2 ones; they are then retained for the subsequent parametric analyses. It's worthy to notice that *sc* ECF^2 values are always higher or equal *oc* ECF^2; therefore, the former indicator can be privileged for its use for VBDI in PE multifunctional composite structures vibrating in *transverse* bending. However, both *sc* and *oc* ECF^2 indicators are not suitable when *in-plane* and *torsion* vibrations are dominant.

4. Damage detection indicators parametric assessment

In order to check the validity of above obtained results for fixed MR and ISL damage characteristics of $[X_d\ L_d\ H_d]$ = [80 5 1.5] mm and [80 5 1] mm, respectively, these parameters are varied according to the values summarized in Table 3. The 3D simulations are then conducted under the previously investigated four mechanical BC of the damaged hybrid composite beams and patches electrodes' two electric connections. It's worth noticing that, for the ISL damage model, the number and thickness of Teflon® layers vary in terms of the damage geometric characteristics.

Model	parameters case	X_d (mm) X_d/L						L_d (mm) L_d/L				H_d (mm) H_d/H		
RM	1			60				5	10	15	20	0.5	1	1.5
				0.3				*0.025*	*0.05*	*0.075*	*0.1*	*0.0125*	*0.25*	*0.375*
	2	60	80	100	120	140	160		5			0.5	1	1.5
		0.3	*0.4*	*0.5*	*0.6*	*0.7*	*0.8*		*0.025*			*0.0125*	*0.25*	*0.375*
	3	60	80	100	120	140	160	5	10	15	20		1.5	
		0.3	*0.4*	*0.5*	*0.6*	*0.7*	*0.8*	*0.025*	*0.05*	*0.075*	*0.1*		*0.375*	
ISL	1			60 (fixed)				5	10	15	20	0.5	1	
				0.3				*0.025*	*0.05*	*0.075*	*0.1*	*0.0125*	*0.25*	
	2	60	80	100	120	140	160		5 (fixed)			0.5	1	
		0.3	*0.4*	*0.5*	*0.6*	*0.7*	*0.8*		*0.025*			*0.0125*	*0.25*	
	3	60	80	100	120	140	160	5	10	15	20		1	
		0.3	*0.4*	*0.5*	*0.6*	*0.7*	*0.8*	*0.025*	*0.05*	*0.075*	*0.1*		*0.25*	

Table 3. Damage characteristics variations for the *parametric analysis* of damaged smart composite beams.

Maximum reached ECF^2 values for the two damage models, four BC and two electric connections are summarized in Table 4. It can be noticed that: (i) RM induced ECF^2 is generally higher than ISL one; (ii) maximum values are obtained for the CS BC under RM damage and for CF BC under the ISL one, with relatively close values but for different modes and damages characteristics; (iii) *sc* and *oc* ECFs reach almost same maximum values for the same modes. Since the *sc* ECF^2 is slightly higher, it is then recommended to choose it as a damage indicator regardless of the damage model.

Damage	Indicator	Characteristics	CF	CS	CC	SS
RM	*sc*	$[X_d, L_d, H_d]$	[140 10 1.5]	[**60 20 1.5**]	[60 10 0.5]	[60 20 1]
		(%, mode)	(-77.31; 5)	(**-80.76**; **2**)	(-73.63; 2)	(28.12; 2)
	oc	$[X_d, L_d, H_d]$	[140 10 1.5]	[**60 20 1.5**]	[60 10 0.5]	[60 20 1]
		(%, mode)	(-77.26; 5)	(**-80.58**; 2)	(-73.58; 2)	(28.01; 2)
ISL	*sc*	$[X_d, L_d, H_d]$	[**120 15 1**]	[160 20 1]	[140 15 1]	[60 20 1]
		(%, mode)	(**73.72**; **8**)	(26.55; 2)	(34.60; 2)	(23.44; 7)
	oc	$[X_d, L_d, H_d]$	[**120 15 1**]	[160 20 1]	[140 15 1]	[60 20 1]
		(%, mode)	(**73.70**; **8**)	(26.53; 2)	(34.59; 2)	(23.26; 7)

Table 4. Damage characteristics of maximum reached ECF indicators.

5. Conclusions and perspectives

This contribution presented short-circuit (*sc*) and open-circuit (*oc*) modal effective squared electromechanical coefficient (EMCC) change factors (ECF^2) for the damage detection in hybrid laminated composite beams using piezoceramic patches integrated in a symmetrical configuration. The structural damage was modeled using a removal of material (RM) model, simulating a notch or crack, and an inclusion of soft layer (ISL) model, simulating a delamination. The proposed damage indicators' performance analysis was investigated using

three-dimensional fully coupled piezoelectric finite elements under four mechanical boundary conditions (BC) and for varying damage geometric characteristics (position, length, height). It was found that the ECF^2 is a much more performant indicator than the recently proposed squared frequency change factor (FCF^2) [11]; in particular, the former was found to be a good alternative to the latter for the ISL damage model where the FCF^2 presented very low values. Besides, it was shown that the popular numerical cantilever and analytical simple support BC are not suitable for investigating theoretically frequency-based RM damage detection since in these cases the changes of modes order and type occur, rendering the obtained results specific and not generalizable to other BC. It is then recommended for numerical analysis, to prefer clamped-clamped BC for these and for practical reasons. As an extension of the present work, the conducted parametric analysis results can be further used for training artificial neural networks in order to reach full quantification (detection, *location* and *sizing*) of damages in piezoelectric multifunctional composites vibrating in *transverse* (out-of-plane) *bending*.

Acknowledgments

The first author would like to thank the support of the *Linz Centre of Mechatronics* (LCM) in the framework of the Austrian COMET-K2 programme.

References

[1] W. Fan and P. Qiao. Vibration-based damage identification methods: a review and comparative study. *Structural Health Monitoring*, 10(1):83-111, 2011.

[2] X. H. Jian, H. S. Tzou, C. J. Lissenden and L. S. Penn. Damage detection by piezoelectric patches in a free vibration method. *Journal of Composite Materials*, 31(4):345-359, 1997.

[3] L. S. Penn, J. R. Jump, M. J. Greenfield and G. E. Blandford. Use of the free-vibration spectrum to detect delamination in thick composites. *Journal of Composite Materials*, 33(1):54-72, 1999.

[4] P. Tan and L. Tong. Delamination detection of composite beams using piezoelectric sensors with evenly distributed electrode strips. *Journal of Composite Materials*, 38(4):321-352, 2004.

[5] J. B. Ihn and F. K. Chang. Pitch-catch active sensing methods in structural health monitoring for aircraft structures. *Structural Health Monitoring*, 7(1):5-19, 2008.

[6] V. Gopal, M. Annamdas and C. K. Soh. Application of electromechanical impedance technique for engineering structures: review and future issues. *Journal of Intelligent Material Systems and Structures*, 21(1): 41-59, 2010.

[7] IEEE Inc. *Standards on piezoelectricity*. ANS/IEEE Std 176–1987, USA, 1988.

[8] A. Benjeddou, S. Vijayakumar and I. Tawfiq. A new damage identification and quantification indicator for piezoelectric advanced composites. In *III European Conference on Computational Mechanics: Solids, Structures and Coupled Problems in Engineering*, Lisbon, 5-9 June 2006.

[9] M. A. Al-Ajmi and A. Benjeddou. Damage indication in smart structures using modal effective electromechanical coupling coefficients. *Smart Materials and Structures*, 17(3): art. n° 035023 (15 pages), 2008.

[10] A. Benjeddou. Approximate evaluation of the modal effective electromechanical coupling coefficient. In B. Dattaguru, S. Gopalakrishnan and V.K. Aatre, Editors, *Multifunctional Material Structures and Systems*, 307-315, Springer, Dordrecht, 2010.

[11] A. Benjeddou, M. Hamdi and S. Ghanmi. Frequency damage indicators for piezoelectric composites. In *International Conference on Smart Structures and Systems*, Jeju (South Korea), 8-12 September 2013.